Surface interactions between two like-charged polyelectrolyte gels

Xiao Wang (王宵)[1] and Wei Hong (洪伟)[2,1,*]
[1]*Department of Materials Science and Engineering, Iowa State University, Ames, Iowa 50011, USA*
[2]*Department of Aerospace Engineering, Iowa State University, Ames, Iowa 50011, USA*
(Received 5 January 2010; revised manuscript received 10 February 2010; published 14 April 2010)

Due to the migration of mobile molecules and ions, a thin diffusive layer of distributed charge—the electric double layer—forms at the interface between a polyelectrolyte gel and a liquid ionic solution. When two polyelectrolyte gels are brought closely together, the electric double layers overlap and interact with each other, resulting in an effective repulsion. The multiphysics-coupling nature of soft gels makes their surface interactions significantly different from the interactions between rigid solids. Using the recently formulated nonlinear theory, this paper develops a continuum model to study the surface interactions between two like-charged polyelectrolyte gels, accounting for the coupled electric, concentration, and deformation fields in both the gels and the liquid. Numerical solutions of the surface interactions are obtained and compared to a qualitative scaling law derived via linearization. The results suggest that the structure of double layers, as well as their interactions, depends not only on the concentration of liquid solutions, but more on the bulk properties of the gels such as stiffness and fixed-charge density. This model also provides insights to the mechanism of the low-friction phenomena on the surface of a polyelectrolyte gel.

DOI: 10.1103/PhysRevE.81.041803 PACS number(s): 82.35.Rs, 68.35.bm, 46.55.+d, 46.25.Hf

I. INTRODUCTION

When a solid is brought into contact with an ionic solution, an electric double layer will form on the solid-liquid interface due to charge separation. A widely accepted model known as the Derjaguin-Landau-Verwey-Overbeek (DLVO) theory [1,2] describes this phenomenon: surface charge accumulates on the solid side while a diffusive charge layer forms in the liquid, without much dependence on the bulk state of the solid. A double layer will also form on the interface between a polyelectrolyte gel and a solution, but exhibit distinct characteristics. Containing a great amount of solvent molecules when swollen, a polyelectrolyte gel encompasses mobile ions and thus the double layer is diffusive on both sides of the interface. In addition, the concentrations of solvent and solutes in a polyelectrolyte gel couple strongly with deformation, making it suitable for stimuli-responsive smart devices [3–7]. Naturally, the double layer is also expected to be influenced by the swelling state of a gel, but the correlation has not yet been fully understood [8].

When two interfaces are brought closer and the free energy of the system increases, the double layers will overlap and create an effective repulsion in between, known as the disjoining pressure. Besides electrostatic interactions, current understanding of surface interactions also accounts for van der Waals forces, as well as steric and depletion effects [8,9]. The double layers are usually very thin and their effects are often seen on microscale particles in systems such as thin films and colloidal suspensions. However, there are cases when double-layer interactions dominate over other factors and become macroscopically appreciable. One prominent example would be the disjoining pressure between two like-charged polyelectrolyte gels in an ionic solution. The repulsion between double layers may be the origin of the low friction between gels [10,11]: when the disjoint pressure is strong enough to balance the normal load, the solution forms a liquid layer in the gap and prevents dry friction. This correlation is strongly supported by the direct measurements of the normal and friction forces between solid surfaces decorated with polyelectrolyte brushes [12–15]. This mechanism is also believed to be essential to understanding the extraordinary lubrication properties of articular cartilages, a type of strongly charged composite polyelectrolyte gels which have a friction coefficient of 10^{-3} even at very low relative speed, while sustaining a compression of up to 10 MPa [16–19].

Due to the multiphysics-coupling nature of polyelectrolyte gels, the disjoining pressure is usually dependent on the seemingly unrelated material properties such as stiffness, deformation state, and ion concentrations. The continuum theory regarding the understanding of the macroscopic electrochemical interactions in a polyelectrolyte gel is still dubious. Some researches extend the theory of porous media to gels [20,21]. Others propose multiphasic models which treat the polymer network, solvent, and mobile ions as separate continuum phases in order to understand the behaviors of polyelectrolyte gels from the viscous drag between the network and solvent [16,17]. A more recent study models the gels as solids with surface charge and calculates the repulsion due the double layers formed between gel surfaces [11]. However, some assumptions drawn directly from studies of rigid impermeable solids may not be justifiable for gels. For example, the electroneutral assumption is no longer tenable inside the double layer on a gel-liquid interface. Although solving the electric field in the liquid independently may be valid for a solid-liquid interface, such an approach disregards the exchange of ions and solvent molecules and is thus not suitable for gel-liquid interfaces.

In this paper, we adopt the recently developed nonlinear field theory for the coupled large deformation and electrochemistry of polyelectrolyte gels [22] in order to study the interactions between the surfaces of two like-charged gels.

*whong@iastate.edu

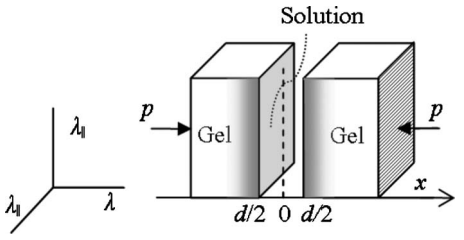

FIG. 1. Schematic representation of the model under consideration. Two thick polyelectrolyte gels, both immersed in an ionic solution, are brought together to a distance of d. Double layers form in the gap and in the gels near the surfaces. The interaction between the double layers induces a repulsion, which could balance the externally applied load p.

Starting from the basic principles of thermodynamics, this approach makes no assumption beyond the material-specific free-energy functions. We simultaneously solve the electric and concentration fields in both the gel and the solution, together with the deformation in the gel, and calculate the disjoining pressure under various circumstances. The dependences of the disjoining pressure on various material and environmental parameters are studied and discussed subsequently.

II. MODEL

A polymeric gel, formed through crosslinking a polymer solution, can swell and deswell reversibly by exchanging solvent with the environment. As a special kind of polymeric gels, the polyelectrolyte gel carries functional groups which dissociate in a solvent and form fixed charges on the network. Naturally, the swelling and deformation of the polyelectrolyte gel are sensitive to the ionic concentrations both in the environment and on its own network. Following Hong *et al.* [22], we adopt a nonlinear field theory to describe the coupling behaviors of a polyelectrolyte gel.

The system under consideration is sketched in Fig. 1. Two identical polyelectrolyte gels, both submerged in a liquid ionic solution, are brought closely together to a distance d so that the double layers will overlap and affect each other. Both gels are swollen and in equilibrium with the external solution. The overall sizes of the gels are much larger than d, therefore we will treat both of them as semi-infinite and model the system as one dimensional. The effect of the surface is also neglected when we are calculating the overall swelling of the gels. The x axis is set at a direction normal to the interfaces and the origin lies on middle plane of the gap between the gels. Due to symmetry, we will only look at half of the system, $0<x<\infty$. The deformation field in a gel is determined by the stretch along x axis, $\lambda(x)$, namely the ratio between the current length and the length in the reference state. Here we will take the dry state of the polymer network as the reference. The lateral stretch parallel to the gap is assumed to be a constant, $\lambda_\parallel$. The directions of the stretches are also shown in Fig. 1. An external pressure p is applied in the x direction to balance the repulsion in between the two gels. Denoting the electric potential as $\Phi(x)$, we will have the electric field $E=-d\Phi/dx$ in both the gel and the solution. In deforming gels, it is often convenient to invoke the nominal electric field defined in the reference state [23], $\tilde{E}=\lambda E$. We take the continuum approach so that no interaction between individual charges needs to be explicitly accounted for. Although the valence of ions will affect the equilibrium swelling ratio of a gel and further the double layers, it is beyond the scope of the current paper and, for simplicity, we will study a system that contains monovalence ions. We assume that the charged groups on the network are fully dissociated so that the nominal concentration of fixed ions C^0 is a constant. Without losing generality, we also assume that the fixed ions are negatively charged. Let $C^+(x)$ and $C^-(x)$ be the nominal concentrations of the mobile counterions and coions. All nominal concentrations are measured with respect to the volume of the dry polymer in the reference state and they are related to the true concentrations as $c^\pm = C^\pm/\lambda\lambda_\parallel^2$.

A. Inhomogeneous fields inside a polyelectrolyte gel

Following Hong *et al.* [22], we extend the Flory-Rehner model [24,25] by writing the free energy per unit reference volume of the gel as

$$W(\lambda,\tilde{E},C^+,C^-) = \frac{G}{2}[\lambda^2+2\lambda_\parallel^2-3-2\ln(\lambda\lambda_\parallel^2)]-\frac{\varepsilon}{2}E^2\lambda\lambda_\parallel^2 + \frac{kT}{v}\left(vC^s\ln\frac{vC^s}{1+vC^s}-\frac{\chi}{1+vC^s}\right) + kTC^+\left(\ln\frac{C^+}{C^s v c_0}-1\right) + kTC^-\left(\ln\frac{C^-}{C^s v c_0}-1\right), \quad (1)$$

where v is the volume of a solvent molecule and that of a unit on a polymer chain, kT is the temperature in the unit of energy, and C^s is the nominal concentration of the solvent. The first term on the right-hand side of Eq. (1) is the free energy of stretching the polymer network, in which a neo-Hookean material law with initial modulus G is adopted. The second term is the Gibbs free energy of polarization, with the assumption that the nonionic solvent and polymer network are both liquidlike ideal dielectrics [26] of permittivity ε. The third term represents the free energy of mixing the solvent with the polymer network [24,27], consisting of both the entropy of mixing and the enthalpy of mixing with the latter characterized by a dimensionless parameter χ. The last two terms are contributions from the solute ions due entirely to the entropy of mixing with the solvent, with c_0 being the reference concentration in a liquid solution at which the chemical potentials of the solutes are set to be 0. Here we will take the concentration in the external solution far from the gel to be the reference for solute chemical potentials. In this paper, we still assume the molecular incompressibility and neglect the volume of the solute ions, so that the volume expansion in the network is fully taken by solvent molecules

$$1+vC^s=\lambda\lambda_\parallel^2. \quad (2)$$

The constitutive relations between the conjugate pairs of field variables can be determined from the partial derivatives of the free-energy function in Eq. (1). The stress along x axis can be given as

$$\sigma = \frac{\partial W(\lambda,\tilde{E},C^+,C^-)}{\lambda_\parallel^2\,\partial\lambda} = \frac{G}{\lambda_\parallel^2}\left(\lambda-\frac{1}{\lambda}\right)+\frac{\varepsilon}{2}E^2+\frac{kT}{v}\left[\ln\left(1-\frac{1}{\lambda\lambda_\parallel^2}\right)+\frac{1}{\lambda\lambda_\parallel^2}+\frac{\chi}{(\lambda\lambda_\parallel^2)^2}-\frac{C^+ + C^-}{C^s}\right], \tag{3}$$

in which the first term is the stress from stretching the polymer network, the second term is the Maxwell stress, and the last term is the contribution from mixing, often referred to as the osmotic pressure. The true electric displacement is related to the electric field as

$$D = -\frac{\partial W(\lambda,\tilde{E},C^+,C^-)}{\lambda_\parallel^2\,\partial\tilde{E}} = \varepsilon E = -\varepsilon\frac{d\Phi}{dx}. \tag{4}$$

The electrochemical potentials of the mobile counterions (+) and coions (−) are, respectively,

$$\mu^\pm = \pm e\Phi + \frac{\partial W(\lambda,\tilde{E},C^+,C^-)}{\partial C^\pm} = \pm e\Phi + kT\ln\frac{C^\pm}{C^s v c_0}, \tag{5}$$

where e is the elementary charge.

In equilibrium, the stress balances the externally applied load and the boundary condition from the liquid, the electric displacement satisfies Gauss's law

$$\frac{dD}{dx} = e\left(c^+ - c^- - \frac{C^0}{\lambda\lambda_\parallel^2}\right), \tag{6}$$

and the electrochemical potentials of the solute ions equal those in the liquid solution in the far field, i.e., the reference

$$\mu^\pm = 0. \tag{7}$$

Substituting Eq. (5) into Eq. (7), we have the equilibrium concentration of mobile ions in the gel

$$C^\pm = C^s v c_0 \exp(\mp\Psi), \tag{8}$$

where $\Psi = e\Phi/kT$ is the dimensionless electric potential. A combination of Eqs. (4), (6), and (8) further yields the Poisson-Boltzmann equation for the electric field in the gel

$$\frac{d^2\Psi}{d\xi^2} = \frac{1}{\lambda\lambda_\parallel^2}\left[(\lambda\lambda_\parallel^2-1)\sinh\Psi + \frac{C^0}{2c_0}\right], \tag{9}$$

in which $\xi = x/L_D$ is the dimensionless coordinate, with L_D being the Debye length, $L_D = \sqrt{kT\varepsilon/2e^2c_0}$.

Substituting Eq. (8) into Eq. (3), we have

$$\frac{v\sigma}{kT} = \frac{vG}{kT}\frac{1}{\lambda_\parallel^2}\left(\lambda-\frac{1}{\lambda}\right)+\left[\ln\left(1-\frac{1}{\lambda\lambda_\parallel^2}\right)+\frac{1}{\lambda\lambda_\parallel^2}+\frac{\chi}{(\lambda\lambda_\parallel^2)^2}\right] + vc_0\left[\left(\frac{d\Psi}{d\xi}\right)^2 - 2\cosh\Psi\right], \tag{10}$$

where $v\sigma/kT$ and vG/kT are the dimensionless axial stress and modulus, respectively. Equations (9) and (10) form an algebraic-differential system for the coupled normalized electric potential $\Psi(\xi)$ and stretch $\lambda(\xi)$ in the polyelectrolyte gel.

B. Interaction between two double layers

Despite the use of a sharp gel-liquid interface in the model, a transition zone with inhomogeneous but continuous fields at the vicinity of the interface exists in both the gels and the liquid gap. The liquid can be regarded as a limiting case of a polyelectrolyte gel with the network stiffness being 0 and the volume fraction of solvent approaching 1. At such a limit, neither the free energy of stretching nor that of mixing the network and solvent is present. The approach described in Sec. II A is also applicable to a liquid solution, with the exception of the indeterminate deformation field.

In the domain $0<\xi<d/2L_D$, since the space is fully occupied by the liquid solution, the electric field is decoupled from the stress balance and Eq. (9) reduces to

$$\frac{d^2\Psi}{d\xi^2} = \sinh\Psi. \tag{11}$$

Equation (11) can be integrated once into

$$\frac{d\Psi}{d\xi} = \sqrt{2[\cosh\Psi - \cosh\Psi(0)]}. \tag{12}$$

Due to symmetry, the electric field vanishes on the middle plane in the gap between the two gels, where $\xi=0$, and the true stress reduces to

$$\frac{v\sigma}{kT} = -2vc_0\cosh\Psi(0). \tag{13}$$

Similarly, we can also obtain the stress in the solution far from the gap where the electric potential equals 0, $v\sigma_0/kT = -2vc_0$. From a mechanical point of view, the *disjoining pressure* is the difference between the stress in the gap and that in the far field, i.e., the part of stress that balances external mechanical loads, $p=-(\sigma-\sigma_0)$.

Since distributed charge dominates in a double layer, we hereby assume the electric displacement to be continuous across the interface and neglect any surface charge. Given the high swelling ratios of most polyelectrolyte gels, we assume the effective permittivity of the nonionic components in the gel to be the same as that of the liquid solvent. As a result, both the electric potential and its spatial derivative are continuous at the interface, $\xi_d = d/2L_D$. Consequently, Eq. (12) provides a boundary condition to the algebraic-differential system in the gel

$$\left.\frac{d\Psi}{d\xi}\right|_{\xi_d} = \sqrt{2\cosh\Psi(\xi_d) + \frac{\sigma}{kTc_0}}. \tag{14}$$

C. Donnan equilibrium of a swollen gel

On the bulk gel side far from the interface, the electric field vanishes and thus the deformation, as well as the ion

concentrations, of the gel becomes homogenous. The state of the gel recovers that of Donnan equilibrium [17,28] and Eq. (9) reduces to the electric-neutrality condition

$$\sinh \Psi_\infty = -\frac{C^0}{2c_0(\lambda_\infty \lambda_\parallel^2 - 1)}, \tag{15}$$

where λ_∞ is the axial stretch deep inside the gel and Ψ_∞ is the dimensionless *Donnan potential*, namely, the equilibrium electric potential (relative to 0 in the external solution). Eliminating Ψ from Eqs. (10) and (15), we have the axial stress

$$\frac{v\sigma}{kT} = \frac{vG}{kT}\frac{1}{\lambda_\parallel^2}\left(\lambda_\infty - \frac{1}{\lambda_\infty}\right) + \left[\ln\left(1 - \frac{1}{\lambda_\infty \lambda_\parallel^2}\right) + \frac{1}{\lambda_\infty \lambda_\parallel^2} + \frac{\chi}{(\lambda_\infty \lambda_\parallel^2)^2}\right] - v\sqrt{\left(\frac{C^0}{\lambda_\infty \lambda_\parallel^2 - 1}\right)^2 + 4c_0^2}. \tag{16}$$

The lateral stress in the gel also balances that in the solution, $2\sigma_0 \lambda \lambda_\parallel = \partial W / \partial \lambda_\parallel$. Consequently,

$$\frac{vG}{kT}\frac{1}{\lambda_\infty}\left(1 - \frac{1}{\lambda_\parallel^2}\right) + \left[\ln\left(1 - \frac{1}{\lambda_\infty \lambda_\parallel^2}\right) + \frac{1}{\lambda_\infty \lambda_\parallel^2} + \frac{\chi}{(\lambda_\infty \lambda_\parallel^2)^2}\right] - v\sqrt{\left(\frac{C^0}{\lambda_\infty \lambda_\parallel^2 - 1}\right)^2 + 4c_0^2} = -2vc_0. \tag{17}$$

Equation (16) can be written in terms of the disjoining pressure by considering Eq. (17),

$$\frac{p}{G} = \frac{1}{\lambda_\infty} - \frac{\lambda_\infty}{\lambda_\parallel^2}. \tag{18}$$

Under a specific deformation state, the disjoining pressure p and the equilibrium stretches deep in the gel, λ_∞ and $\lambda_\parallel$, can be obtained by solving the nonlinear algebraic systems (17) and (18) simultaneously. The result is further used as the input parameters to the field equations in the double layer, Eqs. (9) and (10). The resulting Donnan potential Ψ_∞ can also be used as the boundary condition for $\Psi(\xi)$ at $\xi \to \infty$. The algebraic-differential system is then solved numerically in the gel domain, with boundary conditions (14) and Ψ_∞. Once the electric potential on the interface $\Psi(\xi_d)$ is evaluated, we can further integrate Eq. (12) to obtain the equilibrium width of the gap between the gels

$$\frac{d}{L_D} = 2\int_{\Psi(0)}^{\Psi(\xi_d)} \frac{d\Psi}{\sqrt{2\cosh \Psi + \frac{\sigma}{kTc_0}}}. \tag{19}$$

III. RESULTS AND DISCUSSION

A. Approximate solution at the low-potential limit

When Donnan potential is relatively low, $\Psi_\infty \ll 1$, from Eq. (15), we have

$$\Psi_\infty \approx -\frac{C^0}{2c_0(\lambda_\infty \lambda_\parallel^2 - 1)}. \tag{20}$$

At such a limit, if we further neglect the inhomogeneity in the deformation near the interface by taking $\lambda \approx \lambda_\infty$ in Eq. (10), we can decouple the differential-algebraic system and linearize Eq. (9) as

$$\frac{d^2\Psi}{d\xi^2} \approx \left(1 - \frac{1}{\lambda_\infty \lambda_\parallel^2}\right)(\Psi - \Psi_\infty). \tag{21}$$

Equation (21) holds in the gel domain, $\xi_d < \xi < \infty$, at the low-potential limit. Similarly in the liquid domain, $0 < \xi < \xi_d$, Eq. (11) is linearized to the Debye-Huckel equation

$$\frac{d^2\Psi}{d\xi^2} \approx \Psi. \tag{22}$$

Integrating Eqs. (21) and (22) directly with the boundary condition $\Psi(\infty) = \Psi_\infty$, we obtain an approximate analytical solution for the electric potential:

$$\Psi \approx \begin{cases} \dfrac{\beta \Psi_\infty \cosh \xi}{\sinh \xi_d + \beta \cosh \xi_d} & (0 < \xi < \xi_d) \\ \dfrac{-\Psi_\infty \sinh \xi_d}{\sinh \xi_d + \beta \cosh \xi_d}\dfrac{\exp(-\beta\xi)}{\exp(-\beta\xi_d)} + \Psi_\infty & (\xi_d < \xi < \infty), \end{cases} \tag{23}$$

where $\beta = \sqrt{1 - 1/\lambda_\infty \lambda_\parallel^2}$.

The solution in Eq. (23) shows the characteristics of the double layers in a gap between two like-charged polyelectrolyte gels. The spatial profile of the electric potential resembles that shown in Fig. 2(a). On each interface, the double layer extends into both the liquid solution and the gel. The influence of the double layers decays exponentially into the gel, with a characteristic length L_D/β, which depends on the equilibrium swelling ratio of the gel. For a highly swollen gel, the part of the double layer inside the gel is similar to that in the liquid, both sharing the same Debye length, L_D.

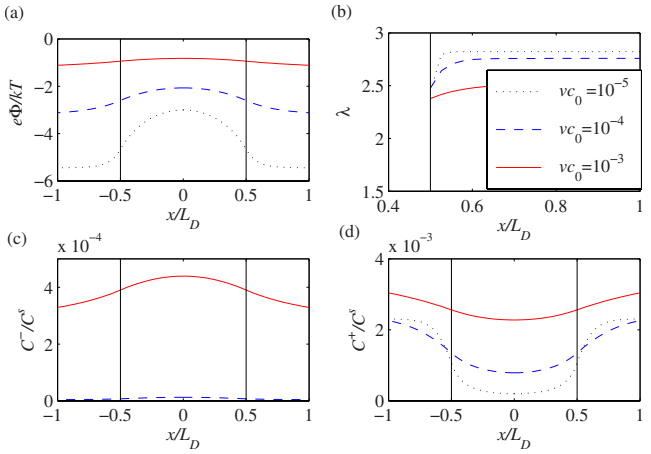

FIG. 2. (Color online) (a) Normalized electric potential in the liquid solution and in the gels near the interfaces. (b) Inhomogeneous axial stretch of the gel near a gel-liquid interface. [(c) and (d)] Concentrations of coions and counterions, respectively, in the gap and in the gels near the interfaces. Vertical solid lines denote the location of the gel-liquid interface. Parameters used in the numerical calculation: normalized stiffness of the gels $vG/kT = 0.01$; molar fraction of fixed charge in the reference state $vC^0 = 0.05$. The gels are submerged in a binary solution of three different concentrations as indicated.

On the other hand, for a very stiff gel that hardly swells, $\beta \approx 0$, Eq. (23) predicts the limit of a conducting solid. However, at such a limit, the Donnan potential is often high and this approximation may not be accurate. A detailed discussion on this limit will be carried out later in Sec. III B.

Using the electric potential on the symmetry plane, $\Psi(0)$, we can further identify the relation between the disjoining pressure and the gap width using Eq. (13)

$$\frac{\upsilon p}{kT} \approx 2\upsilon c_0 \left[\cosh \frac{\beta \Psi_\infty \exp(-\xi_d)}{\sinh \xi_d + \beta \cosh \xi_d} - 1 \right]. \tag{24}$$

In the case when the gel is highly swollen, $\beta \approx 1$, Eq. (24) can be further simplified into

$$\frac{\upsilon p}{kT} \approx \upsilon c_0 \Psi_\infty^2 \exp(-2\xi_d). \tag{25}$$

Equation (25) provides an approximate scaling law that characterizes the dependence of the disjoining pressure on Donnan potential, the gap width, and the ion concentration in the external solution. Although not shown explicitly in Eq. (25), the bulk properties of the polyelectrolyte gels (e.g., stiffness and fixed-ion concentration) also affect the disjoining pressure through changing Donnan potential. In more general parameter ranges other than the low-potential limit, the validity of this scaling law will be checked by comparing to the numerical calculations as follows.

B. Structure of overlapping double layers

Following the procedure described in Sec. II B, we solve the nonlinear system numerically. To enable calculations, we set the dimensionless stiffness of the polymer network $\upsilon G/kT = 0.01$, corresponding to a modulus of $\sim 10^5$ Pa at room temperature when the solvent is water. We also set the nominal fixed-ion density $\upsilon C^0 = 0.05$, corresponding to a 5% molar fraction of charge-carrying monomers on the network. To demonstrate the interactions between the overlapping double layers, solutions to the cases when the disjoining pressure is in equilibrium with the external load at a gap width of 1 D length are presented here.

Figure 2 plots the spatial profile of the field variables in the liquid domain and the gel domain near the interfaces of two polyelectrolyte gels that are immersed in solutions of various concentrations, $\upsilon c_0 = 10^{-3}$, 10^{-4}, and 10^{-5}. In the near-interface regions, the distributions of the electric potential, axial stretch, and concentration are all inhomogeneous. The gel and the liquid solution are no longer electroneutral: ions diffuse through the gel-fluid interface and result in a negatively charged layer in the gel and a positively charged layer in the liquid. As shown in Fig. 2(a), the electric potential decays exponentially into the gels and approaches the Donnan potential. This agrees qualitatively with the prediction of the approximate solution in Eq. (23).

Plotted in Fig. 2(b) is the stretch along the x axis in a polymeric gel. Corresponding to the inhomogeneity in the electric potential, loss of counterions in a gel near the interface breaks the swelling equilibrium and the polymer network stretches less compared to the bulk. In the depth direction, the stretch is smaller as shown in Fig. 2(b). Along the interface, the surface layer is constrained by the bulk and a tensile surface stress is thus developed. Such a stress has little contribution to the surface interactions and is thus not shown here. On the other hand, the effect of the ion imbalance on the axial stretch is determined by volume fraction of solvent. In a dilute external solution, the fixed ions on the network become more prominent and the stronger effect will result in a more inhomogeneous deformation.

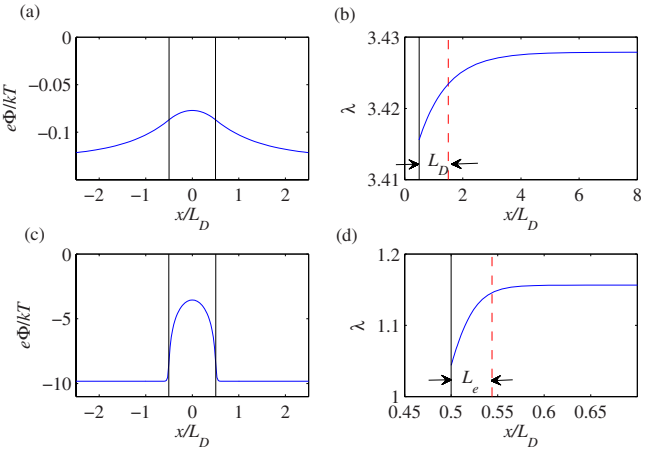

FIG. 3. (Color online) Equilibrium profiles of the normalized electric potential and axial stretch in a gel in the cases of [(a) and (b)] relatively compliant gels with dimensionless modulus $G\upsilon/kT = 10^{-3}$ and fixed-charge density $\upsilon C^0 = 0.01$ and [(c) and (d)] relatively stiff and strongly charged gels with $G\upsilon/kT = 10$ and $\upsilon C^0 = 1$. The gels are submerged in a binary solution of concentration $\upsilon c_0 = 10^{-3}$ in both cases. The fields in the compliant gels show a characteristic length close to the Debye length L_D, while those in the stiff gels show a much smaller characteristic length $L_e = \sqrt{\varepsilon \Phi_\infty^e / G}$. Vertical solid lines denote the location of the gel-liquid interface.

As can be seen on the plots in Fig. 2, the penetration depth, namely, the thickness of the diffusive layer in the gel where the fields are inhomogeneous, is no longer the Debye length, but depends on various parameters including the equilibrium swelling ratio and mobile-ion concentrations. There are three major energy contributions in the system: the elastic energy of the network which scales with the modulus G, the electrostatic energy which scales with εE^2, and the entropic thermal energy which scales with kT. To understand the mechanism, we further look at the following two limiting cases. When the network is relatively compliant, $\upsilon G/kT \ll 1$, the electrostatic energy and the thermal energy dominate over the elastic energy and balance each other in the inhomogeneous layer. As shown in Figs. 3(a) and 3(b), just as in a liquid, the inhomogeneous layer in the gel also has a characteristic length comparable to the Debye length, which results from the competition between the electrostatic energy and the thermal fluctuation. When the network is relatively stiff ($\upsilon G/kT \gg 1$), Donnan potential is high under a relatively low external concentration ($\upsilon c_0 \ll C^0/C^s$) and the electrostatic energy is balanced by the elastic energy. The competition between the elastic energy in the polymer network and the electrostatic energy gives rise to a new characteristic length

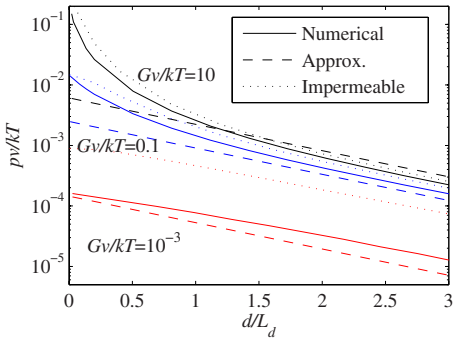

FIG. 4. (Color online) Disjoining pressure as a function of the gap width between two like-charged polyelectrolyte gels with fixed-charge density $vC^0=0.05$ and external ion concentration $vc_0=10^{-4}$. Three curves are plotted for each case of the three different stiffness values: (1) numerical solutions to the nonlinear differential-algebraic system in Eqs. (9) and (10), (2) the approximate exponential relation given by Eq. (25) at a low-potential limit, and (3) the solution to the approximate model in which the gels are modeled as impermeable solid with charge accumulates only on the surface.

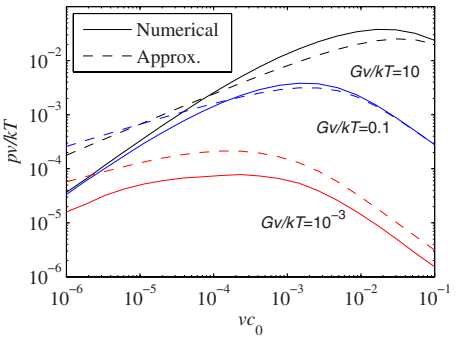

FIG. 5. (Color online) Normalized disjoining pressure between two like-charged gels separated at 1 Debye length as a function of the molar fraction of solute in the external solution. The molar fraction of the fixed ions in the reference state is $vC^0=0.05$. The numerical solutions to the rigorous differential-algebraic system are plotted as solid curves and the analytical approximations at low Donnan potentials are plotted as dashed curves.

$$L_e = \sqrt{\frac{\varepsilon\Phi_\infty^2}{G}}. \tag{26}$$

As shown in Figs. 3(c) and 3(d), the inhomogeneous fields in the gels decay at a depth comparable to L_e and much smaller than L_D. In the limit of a rigid solid, $L_e \to 0$, our model recovers the classical picture of the double layer on a solid-liquid interface: the charge in the solid only concentrates on its surface.

C. Disjoining pressure as a function of the gap width

The interaction energy between the double layers increases when two polyelectrolyte gels approach to each other and the excess in the total free-energy gives rise to the disjoining pressure. The origin of the disjoining pressure between two gel surfaces is similar to that between two solid surfaces [9], although the behavior is different. We plot the results of the normalized disjoining pressure, pv/kT, as a function of the dimensionless gap width d/L_D in Fig. 4. The numerical solutions to the nonlinear differential-algebraic system are plotted together with the approximate solution at the low-potential limit, Eq. (25). As can be seen in Fig. 4, the exponential dependence of the disjoining pressure on the gap width agrees qualitatively well with the numerical solutions, especially when the network stiffness is relatively low and the gels are not too close. The deviation from the low-potential approximate is greater when the gel is stiffer. The dependency of the disjoining pressure on the gap width obtained here also agrees with that measured experimentally between two solid surfaces bearing polyelectrolyte brushes [13–15], although the influence in the material properties has not been fully revealed in the experiments due to the constraint from the rigid substrate.

For comparison, we also plot the solution to an approximate model in which the gels are taken to be impermeable solids (the dotted curves in Fig. 4), i.e., the charge in a gel exists only on the surface [9]. The equilibrium Donnan potential in the gel is used as the surface potential in this approximate. The solid-liquid model and our gel-liquid model show a very similar trend in the gap-width dependence of the disjoining pressure, although the quantitative predictions can differ by 1 order of magnitude. From the plots shown on Fig. 4, one might be able to obtain a better approximate by assuming an effective gap width slightly larger than the distance between the gels. It is physically sensible since the double layers now also extend to a finite depth into the gels. However, it may be impractical because the effective increase in the gap width and the surface potential depend on the local deformation state of the gel and the ion concentrations.

D. Dependence of the disjoining pressure on various parameters

One unique feature of the double-layer interaction between polyelectrolyte gels is its dependence on material parameters (e.g., the network stiffness G and the fixed-charge density C^0) as well as the environmental conditions (e.g., the ion concentration of the external solution c_0). Using the rigorous model and the approximate scaling law developed in previous sections, we will study the dependence of the disjoining pressure on all these parameters. Since its dependence on the gap width has already been explored in Sec. III C, the disjoining pressure shown below is evaluated at a gap width of one Debye length.

Figure 5 plots the disjoining pressure as a function of the molar fraction of solute in the external solution, vc_0. The gels with three different network stiffness values, $Gv/kT = 10$, 0.1, 0.001, are calculated and the numerical results and the low-potential linearization, Eq. (24), are shown side by side. The fixed-charge density with respect to the reference (dry) state is set at $vC^0=0.05$. However, the true molar fractions of fixed charge at the current state, C^0/C^s, are different because the equilibrium swelling ratio of a polyelectrolyte gel is determined by the stiffness and the external ion concentration. As shown in Fig. 5, the disjoining pressure first increases with the external ion concentration and then de-

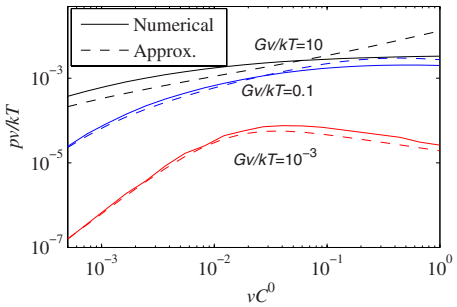

FIG. 6. (Color online) Normalized disjoining pressure between two like-charged gels separated at 1 Debye length, as a function of the fixed-charge density in the reference (dry) state. The molar fraction of the solute in the external solution is kept at $vc_0=10^{-4}$. The numerical solutions to the rigorous differential-algebraic system, Eqs. (9) and (10), are plotted as solid curves, while the analytical approximations at low Donnan potentials, Eq. (25), are plotted as dashed curves.

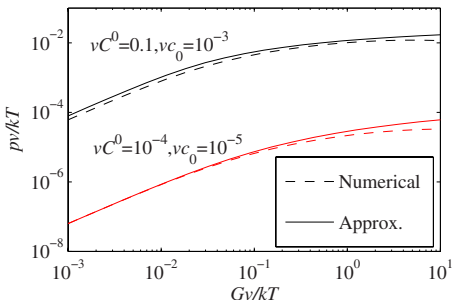

FIG. 7. (Color online) Normalized disjoining pressure pv/kT as a function of the gel stiffness Gv/kT between two like-charged polyelectrolyte gels kept at 1 Debye length apart. Two different combinations of the fixed and external ion concentrations are shown. The numerical solutions to the rigorous differential-algebraic system, Eqs. (9) and (10), are plotted as solid curves and the analytical approximations at low Donnan potentials, Eq. (25), are plotted as dashed curves.

creases after reaching a peak at a certain value of vc_0. The two limiting cases can be understood as follows. When the external solution has a very low ion concentration, the availability of ions in the gap is also limited. Due to the low absolute value of ion concentration, the osmotic pressure induced by the concentration difference will be low, even though a significant difference is present between the concentration in the gap and that in the far field. When the external solution has a very high ion concentration, the fixed ions in the gels are less effective in tuning the ion concentrations in the gap. Even though the ion concentration in the gap is high, it is not too different from that in the far field and thus the resulting osmotic pressure is also low. The value of the external ion concentration, vc_0, at which the disjoining pressure reaches a maximum, is on the same order of the true concentration of the fixed ions in the swollen gels, C^0/C^s. Although no direct experimental evidence has been reported, the positive correlation between the disjoining pressure and the external ion concentration agrees qualitatively with the observation in a closely related experiment on solid surfaces coated with polyelectrolyte brushes [12], especially for the case of relatively high network stiffness.

A similar trend can be seen on the dependence of the disjoining pressure on the fixed-ion concentration, as plotted in Fig. 6. Here, the molar fraction of solute in the external solution is taken to be 10^{-4}. The same arguments of the two limiting cases could be used to rationalize the trend. However, in terms of the nominal concentration of the fixed ions, the value at which the disjoining pressure reaches a maximum is much higher than the external ion concentration. The maximum here is no longer located at the place where the true concentrations of the fixed ions are comparable to that of the ions in the external solution. Instead, for a relatively stiff gel, although the equilibrium swelling ratio is low, the disjoining pressure peaks at a fixed-ion density $vC^0 \sim 1$. At such a high fixed-ion concentration, our free-energy function is arguably valid, but the qualitative trend predicted by the current model shall still hold. A more realist free-energy function capable of characterizing the behavior of the gel with high ion concentrations may provide more accurate quantitative predictions.

Finally, the dependence of the disjoining pressure on the network stiffness is shown in Fig. 7. As plotted in the figure, the disjoining pressure is a monotonically increasing function of the modulus. When the gel is relatively complaint, $Gv/kT \ll 1$, the disjoining pressure is almost linearly proportional to the modulus, $p \propto G$. When the gel is relatively stiff, $Gv/kT > 0.1$, although the disjoining pressure still increases with the stiffness, the accretion is less significant. Moreover, at the limit of a very stiff gel, $Gv/kT \gg 1$, the Donnan equilibrium described by Eq. (15) no longer exists and the disjoining pressure is determined by the surface potential of the material rather than its bulk properties.

It can be seen in Figs. 5–7 that the approximate scaling law captures the qualitative behavior of the disjoining pressure quite well, especially when Donnan potential is low, i.e., when the gel has a low fixed-ion density and a compliant network. Inspired by the approximate Eqs. (24) and (25), we further plot the disjoining pressure as a function of the normalized Donnan potential, Ψ_∞, in Fig. 8. The external ion concentration vc_0 is fixed at 10^{-3}, while a wide range of Gv/kT (10^{-3}, 10^{-2}, …, 10) and vC^0 (10^{-4}, 10^{-3}, …, 1) combinations is calculated. Different combinations of Gv/kT and vC^0 may give the same Donnan potential. The disjoining pressures at three gap widths are calculated for each parameter combination. The results of 25 different parameter combinations are categorized into four groups based on the network stiffness and the fixed-ion concentration: (1) soft ($Gv/kT < 0.1$) and weak ($vC^0 < 0.01$) gels; (2) soft ($Gv/kT < 0.1$) and strong ($vC^0 \geq 0.01$) gels; (3) stiff ($Gv/kT \geq 0.1$) and weak ($vC^0 < 0.01$) gels; (4) stiff ($Gv/kT \geq 0.1$) and strong ($vC^0 \geq 0.01$) gels. From the survey of the wide range of data in Fig. 8, we can see that the approximate scaling law, Eq. (25), agrees well with the rigorous results of the model. Some deviations are expected for very stiff and/or highly charged gels, but the scaling law is still able to capture the qualitative trend.

E. Friction between two like-charged polyelectrolyte gels

Due to its capability of withstanding external loads, the disjoining pressure in the gap between two like-charged

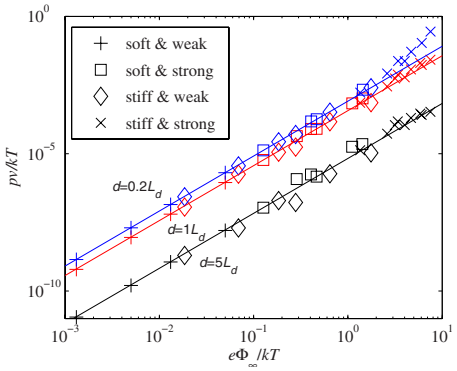

FIG. 8. (Color online) Disjoining pressure of various material-parameter combinations, shown against the dimensionless Donnan potential. A wide range of polyelectrolyte gels, with stiffness $Gv/kT=10^{-3}\sim10$ and fixed-ion concentration $vC^0=10^{-4}\sim1$, has been surveyed. The 25 data points are categorized into four groups: (1) soft ($Gv/kT<0.1$) and weak ($vC^0<0.01$) gels; (2) soft ($Gv/kT<0.1$) and strong ($vC^0\geq0.01$) gels; (3) stiff ($Gv/kT\geq0.1$) and weak ($vC^0<0.01$) gels; (4) stiff ($Gv/kT\geq0.1$) and strong ($vC^0\geq0.01$) gels.

polyelectrolyte gels could play an important role in reducing the friction. When the disjoining pressure separates the two gel surfaces apart with a distance d, the gap is filled with liquid solution that prevents a direct contact of the surfaces. As a result, the only source of friction is from the viscosity of the liquid layer. Assuming the fluid to be Newtonian with viscosity μ, we have the shear stress

$$\tau_f = \frac{\mu v}{d}, \tag{27}$$

where v is the relative speed of sliding. Substituting the approximate scaling law Eq. (25) into Eq. (27), we can further write the shear stress as

$$\tau_f \approx \frac{\mu v}{2L_D}\left(\ln\frac{c_0 e^2\Phi_\infty^2}{pkT}\right)^{-1}. \tag{28}$$

Equation (28) is plotted schematically in Fig. 9. The frictional shear stress diverges when the normal pressure reaches a critical value p_{cr}—the liquid interlayer vanishes and the two surfaces contact. It is worth mentioning that a contact may occur earlier than the critical point due to other factors such as the finite roughness of the surfaces. Using the scaling law of linear approximate, we can estimate the critical pressure as

$$p_{cr} \approx \frac{c_0 e^2\Phi_\infty^2}{kT}. \tag{29}$$

When a normal pressure below the critical value is applied, the friction between the gels is very low and dependent on the speed of relative sliding. Beyond the critical pressure, a much higher dry friction would dominate between the two gel surfaces in physical contact. A dramatic increase in the friction force is expected near the critical pressure level. As discussed in Sec. III D, the critical pressure will depend on

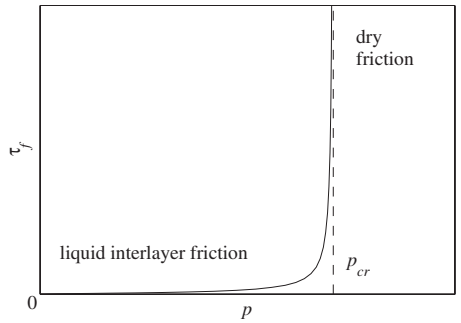

FIG. 9. Schematic plot of the relation between the frictional shear stress τ_f and the normal pressure p. Below a critical value p_{cr}, the applied normal pressure can be balanced by the disjoining pressure and the two polyelectrolyte gels are separated by a liquid interlayer. The friction is mainly caused by the viscosity of the fluid. The friction increases dramatically near the critical pressure, p_{cr}, and transitions to the regular Coulomb friction when the gel surfaces are in contact.

the bulk properties of the polyelectrolyte gels (e.g., stiffness, fixed-charge density) and the environmental parameters such as the concentration of external solution.

Here, for simplicity, we have used the nonslip boundary condition on the gel-liquid interface while deriving Eq. (27). Since the gel contains a polymer network and mobile solvent molecules, a continuous velocity profile of the solvent is also expected in the gel [29,30], just as the electric double layer. The consideration of the flow in the gel will effectively increase the thickness of the liquid gap [10], but will not affect the qualitative predictions. The detailed discussion on this issue is beyond the scope of the current paper.

IV. CONCLUSIONS

Using a continuum model that couples the large deformation and the electrochemistry of polyelectrolyte gels, we have investigated the electrochemomechanical interactions between the surfaces of two like-charged polyelectrolyte gels. When immersed in an ionic solution, the electrolyte groups on the gel network dissociate and form immobile charges. Even though the majority of the fixed charges inside a bulk gel are balanced by the mobile counterions, neither the liquid nor the gel is electroneutral near the interface: an electric double layer forms at the interface and extends into both the liquid and the gel. When two surfaces are brought close together, the electric double layers overlap and change their structure. The excessive energy associated with the change in the double layers gives rise to the disjoining pressure between the two surfaces. The interaction becomes appreciable when the distance between the two surfaces is comparable to the Debye length, a characteristic length of the double layer in the liquid solution. Through linearization, we obtain an approximate scaling law, which implies that the disjoining pressure decays exponentially with the width of the liquid gap and scales with the squared of the equilibrium Donnan potential deep inside the gels. Numerical calculations further confirm the approximate relation. Both the numerical results and the scaling behavior agree qualitatively

with existing experimental measurements. The disjoining pressure also provides a clue to the low-friction phenomena of polyelectrolyte gels. When the applied normal pressure is below a critical value so that it can be balanced by the disjoining pressure, the liquid interlayer prevents the surfaces from direct contact and significantly reduces the friction.

Unlike the double-layer interactions between two solid surfaces, the surface interactions between two polyelelctrolyte gels depend not only on the concentrations of fixed and mobile ions, but also on the bulk properties of the gels. Our model reveals the intricate dependence of the disjoining pressure on material and environmental parameters including the network modulus, the fixed-charge density, and the solute concentration of the external solution. In summary, the model suggests the following requirements for a polyelelctrolyte gel to be optimized for higher disjoining pressure and lower friction: a stiff-enough network with the modulus comparable to kT/v, a very high density of charged groups on the network, and a moderate concentration of external ionic solution which is comparable to the concentration of the fixed ions in the gel when swollen. Interestingly, the articular cartilage, a natural material which is believed to function as a load bearer and friction reducer, seems to fit these descriptions well.

ACKNOWLEDGMENT

The authors acknowledge the supoprt from the National Science Foundation under Grant No. CMMI-0900342.

[1] B. Derjaguin and L. Landau, Prog. Surf. Sci. **43**, 30 (1993); [originally published in Acta Physicochim. URSS **14**, 633 (1941)].
[2] E. J. W. Verwey and J. Th. G. Overbeek, *Theory of the Stability of Lyophobic Colloids* (Elsevier, Amsterdam, 1948).
[3] Y. Osada, H. Okuzaki, and H. Hori, Nature (London) **355**, 242 (1992).
[4] K. Takada, N. Tanaka, and T. Tatsuma, J. Electroanal. Chem. **585**, 120 (2005).
[5] L. Dong, A. K. Agarwal, D. J. Beebe, and H. R. Jiang, Nature (London) **442**, 551 (2006).
[6] K. Ueno, J. Sakamoto, Y. Takeoka, and M. Watanabe, J. Mater. Chem. **19**, 4778 (2009).
[7] A. Sidorenko, T. Krupenkin, A. Taylor, P. Fratzl, and J. Aizenberg, Science **315**, 487 (2007).
[8] B. R. Saunders, N. Laajam, E. Daly, S. Teow, X. H. Hu, and R. Stepto, Adv. Colloid Interface Sci. **147**, 251 (2009).
[9] B. V. Derjarguin, *Theory of Stability of Colloids and Thin Films* (Springer, New York, 1989).
[10] J. P. Gong, G. Kagata, and Y. Osada, J. Phys. Chem. B **103**, 6007 (1999).
[11] J. P. Gong and Y. Osada, Prog. Polym. Sci. **27**, 3 (2002).
[12] M. Balastre, F. Li, P. Schorr, J. Yang, J. W. Mays, and M. V. Tirrell, Macromolecules **35**, 9480 (2002).
[13] U. Raviv, S. Giasson, N. Kampf, J.-F. Gohy, R. Jerome, and J. Klein, Nature (London) **425**, 163 (2003).
[14] U. Raviv, S. Giasson, N. Kampf, J.-F. Gohy, R. Jerome, and J. Klein, Langmuir **24**, 8678 (2008).
[15] I. E. Dunlop, W. H. Briscoe, S. Titmuss, R. M. J. Jacobs, V. L. Osborne, S. Edmondson, W. T. S. Huck, and J. Klein, J. Phys. Chem. B **113**, 3947 (2009).
[16] V. C. Mow, S. C. Kuei, W. M. Lai, and C. G. Armstrong, J. Biomech. Eng. **102**, 73 (1980).
[17] W. M. Lai, J. S. Hou, and V. C. Mow, J. Biomech. Eng. **113**, 245 (1991).
[18] G. A. Ateshian, H. Q. Wang, and W. M. Lai, J. Tribol. **120**, 241 (1998).
[19] G. A. Ateshian, J. Biomech. **42**, 1163 (2009).
[20] H. Ohshima and T. Kondo, J. Colloid Interface Sci. **155**, 499 (1993).
[21] N. I. Zharkikh and S. S. Dukhin, Colloid J. Russ. Acad. **56**, 767 (1994); Colloid J. **56**, 680 (1994).
[22] W. Hong, X. Zhao, and Z. Suo, J. Mech. Phys. Solids **58**, 558 (2010).
[23] Z. Suo, X. Zhao, and W. H. Greene, J. Mech. Phys. Solids **56**, 467 (2008).
[24] P. J. Flory, J. Chem. Phys. **10**, 51 (1942).
[25] P. J. Flory and J. Rehner, J. Chem. Phys. **11**, 521 (1943).
[26] X. H. Zhao, W. Hong, and Z. G. Suo, Phys. Rev. B **76**, 134113 (2007).
[27] M. L. Huggins, J. Phys. Chem. **46**, 151 (1942).
[28] F. G. Donnan, Chem. Rev. **1**, 73 (1924).
[29] H. C. Brinkman, Physica (Amsterdam) **13**, 447 (1947).
[30] C. R. Ethier and R. D. Kamm, PCH, PhysicoChem. Hydrodyn. **11**, 219 (1989).